AIP | Review of Scientific Instruments

# Perturbations induced by electrostatic probe in the discharge of Hall thrusters

L. Grimaud, A. Pétin, J. Vaudolon, and S. Mazouffre

Citation: Review of Scientific Instruments **87**, 043506 (2016); doi: 10.1063/1.4945563
View online: http://dx.doi.org/10.1063/1.4945563
View Table of Contents: http://scitation.aip.org/content/aip/journal/rsi/87/4?ver=pdfcov
Published by the AIP Publishing

REVIEW OF SCIENTIFIC INSTRUMENTS **87**, 043506 (2016)

# Perturbations induced by electrostatic probe in the discharge of Hall thrusters

L. Grimaud, A. Pétin, J. Vaudolon, and S. Mazouffre
*ICARE, CNRS, Orléans 45100, France*

(Received 5 October 2015; accepted 23 March 2016; published online 11 April 2016)

Emissive and Langmuir probes are two widely used plasma diagnostic techniques that, when used properly, give access to a wide range of information on the plasma's ions and electrons. We show here that their use in small and medium power Hall thrusters produces large perturbations in the discharge characteristics. Potential measurements performed by both probes and non-invasive Laser Induced Fluorescence (LIF) spectroscopy highlight significant discrepancies in the discharge profile. This phenomenon is observed both in the 200 W and the 1.5 kW-class thrusters. In order to have a better understanding of these perturbations, ion velocity distribution functions are acquired by LIF spectroscopy at different positions in the smaller thruster, with and without the probes. Emissive probes are shown to produce the biggest perturbation, shifting the acceleration region upstream. The probe insertion is also shown to have significant effect on both the average discharge current, increasing it by as much as 30%, and its harmonic content in both amplitude and spectrum. These perturbations appear as the probe tip passes a threshold located between 0 and 5 mm downstream of the thruster exit plane.  [http://dx.doi.org/10.1063/1.4945563]

## I. INTRODUCTION AND PURPOSE

Hall thrusters (HTs) are one of the most widely used type of electrostatic ion thrusters.[1] Their good thrust to power ratio for electric thrusters and high specific impulse compared to chemical thrusters make them attractive for satellites station-keeping and orbit raising applications. They work by having electrons from a discharge go through a magnetic barrier. The ExB drift induced by the radial magnetic field causes a Hall current to form azimuthally in the annular discharge chamber. This strong current is responsible for the ionization of the neutral xenon propellant injected at the back the channel. High plasma resistivity due to the magnetic field in the region causes a local electric field to form. The resulting electric field accelerates the ions to several kilometers per second and produces thrust.[2,3] The study of the electric field is thus essential to understand the inner workings of the thruster.

Moreover, while particle in cell (PIC) type codes have made great progress over the years, they are still not able to capture all of the discharge characteristics in HT.[4] Their limitation comes both from the available computing power and lack of fine knowledge of the plasma physics, particularly the plasma/wall interface and the so-called "anomalous transport." Knowing the electronic properties of the plasma inside the thruster is one of the primary axes of study for HT, both for simulation validation and performance optimization. In fact numerical models are often adjusted to fit the measured data provided by the experimentalist community. It is thus crucial for that reference data to be as error free as possible.

Measurement in the plume and more generally outside of the thruster channel have been the object of many articles.[5–10] Comparisons between probing methods can also be found in the literature,[10] and while non-intrusive methods have been able to resolve phenomenon which are not picked up by electrostatic probes, the probe perturbations do not appear to be significantly affecting the plasma. However probe measurement inside the thruster itself is more complicated and scarcer.[11–14] High particle flux and density warrant special precautions. Ablation of the ceramic insulators being one of the main identified perturbation causes, several investigators have chosen to use small probes with low residence time inside the thruster. Nevertheless, even with those techniques, it is currently unreasonable to consider probe-induced disturbances in the channel of Hall thruster as negligible. In this article, we compare measurements done by emissive probe (EP) and Langmuir probe (LP) to ones done with Laser Induced Fluorescence (LIF) spectroscopy. We also investigate how the former perturbs the latter. The measurement errors caused by the non-constant magnetic field along the thruster's axis are not considered here. While they are known[15,16] to cause deviations, the application of electrostatic probe theory in magnetic fields was considered too complex for this study. Besides, the probe was positioned perpendicular to the magnetic field lines, which decreases the impact of the magnetic field on the I-V curve.

Emissive probes are a well known type of electrostatic probes widely used to measure plasma potentials in a large variety of discharges, from high temperature, high density to low pressure, low temperature. The traditional method often referred to as the "floating point" technique consists of heating a filament until the thermionic emissions nearly cancel out the plasma sheath around the material. The potential of the probe at this point is close to the plasma potential. The difference between the measured plasma potential is a function of the electron temperature. Several corrections have been proposed to account for space-charge, geometric, and emitted electron energy distribution functions effects.[17–19] For example, thermionic electron emissions introduce additional charged particles with different temperatures and velocities likely to disturb the original discharge. A correction of +1.5 to +2 $T_e/e$

 

is often recommended on the plasma potential measured by the floating point method. While this correction does produce more accurate results, it was not used in this work as our aim was not an accurate measurement of the electric field but a estimation of probe perturbations.

Langmuir probes work by sweeping the potential of a conductor across a predefined range. The current collected by the probe lets us directly get the floating potential as well as plasma potential, electron temperature, and electron density after some post-processing.[20,21] Similarly current drawn by the probe from the surrounding plasma could be one perturbing phenomenon in action.

To examine the influence of the probe insertion, heating, and potential sweep of its tip, we chose to compare their measurements with LIF spectroscopy. This non-intrusive method measures the ion velocity distribution function (IVDF) by looking at fluorescent ions excited by a laser.[22] From this the potential drop experienced by the ions is deduced and we can obtain an electric field distribution that we will compare with probe measurements.

In this article, we will first present the experimental setup with the facilities, thrusters, and probes used as well as the LIF spectroscopy system. A comparison of the potential and electric fields measured by emissive and Langmuir probes as well as LIF is done for different thrusters and channel materials. We then attempt to identify the probe perturbations by comparing local measurement of the IVDF with and without probes. Lastly the influence of the probes on the discharge current value and dynamics is noted.

## II. EXPERIMENTAL SETUP

### A. Thrusters

In this study, two different thrusters have been used.

The PPI (French for Petit Propulseur Innovant) is a 200 W laboratory Hall thruster that has been extensively studied at ICARE.[23] It delivers 10 mN of thrust at a 250 V operating voltage and an anode mass flow rate of 1 mg/s of xenon. The thruster can be fitted with a set of interchangeable ceramic channel walls allowing to change both materials and channel width. This study is done at fixed width but with both $Al_2O_3$ and BN-$SiO_2$ walls. The geometry chosen is our so-called 2S0 configuration corresponding to twice the SPT-100 channel width to diameter ratio. In this case, the channel is 10 mm wide. In this configuration, the magnetic field along the center of the discharge channel peaks at 250 G near the exit plane. This thruster was fired inside the NExET vacuum chamber.[24] The cylindrical $1.5 \times 0.8$ m stainless steel chamber is typically kept around $5 \times 10^{-5}$ mbar background pressure when firing, thanks to a combination of primary, turbo-molecular, and cryogenic pump kept at 38 K.

The SPT-100-ML[25] is a 1.5 kW thruster derived from the Russian SPT-100.[26] This medium size thruster can produce about 80 mN of thrust at an operating voltage of 300 V and an anode mass flow rate of 5 mg/s of xenon. On this thruster, the discharge channel is made out of BN-$SiO_2$. The magnetic field reaches 150 G near the exit plane at the center of the discharge channel. Moreover a slot has been machined on the external wall and a hole was drilled at the back of the channel to allow optical probing of the inside of the thruster. The SPT-100-ML was mounted in the much larger Pivoine-2g test facility.[25] Pivoine-2g consists of a $4 \times 2.2$ m cylindrical vacuum chamber equipped with a dry pump, a turbo-molecular pump, and an array of cryogenic pumps maintaining a background pressure of $10^{-5}$ mbar during thruster operation.

Both those thrusters are operated with a heated MIREA type $LaB_6$ cathode. The cathode mass flow rate was 0.2 mg/s of xenon for the PPI and 0.4 mg/s for the SPT-100-ML.

In both cases, the body of the vacuum chamber is grounded.

### B. Electrostatic probes

The emissive probes used are made in-house and consists of a loop of thoriated tungsten wire crimped at both ends into fine copper tubes. These copper tubes are insulated from the plasma by an surrounding alumina tube. The size of each element can be seen in Figure 1. The heating current going through the filament is controlled by a E3633A Agilent power supply. To keep the probe potential floating with respect to the ground the power supply is isolated with an isolator-transformer.[27] The probe voltage is recorded by an oscilloscope.

Since emissive probes work by canceling the plasma sheath with thermionic emissions, the temperature of the tip and thus the heating current are crucial parameters. When a sufficient flux of electrons is emitted, the sheath surrounding the thoriated tungsten wire is nearly neutralized and the probe potential becomes the plasma potential. The difference in electron temperature between the emitted and ambient electrons means that a dependence on $T_e$ exists. As explained in Section I, this $T_e$ correction was not taken into account in this work. Figure 2 shows the effect of the heating current on the measured potential inside the PPI operated at 200 V and 0.86 A discharge parameters for an anode mass flow rate of 1 mg/s. This figure highlights the fact that the appropriate heating current depends on the plasma characteristics. A rather sharp behavior change is visible around 4 A in the regions of higher electron temperature inside the discharge channel. In accordance to this results, a heating current of 4.4 A was used throughout this work.

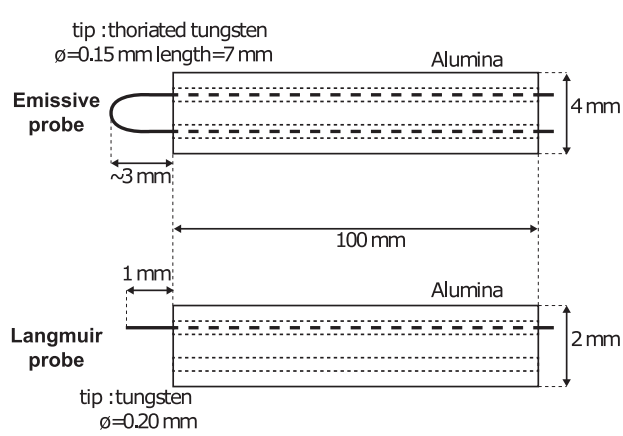


FIG. 1. Electrostatic probe geometry.

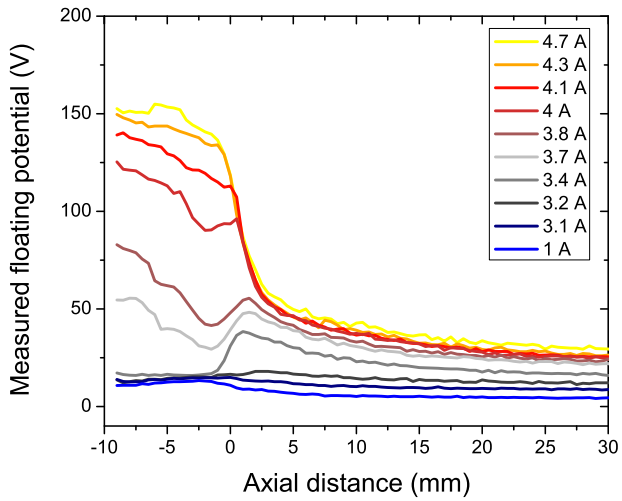


FIG. 2. Floating potential measured along the PPI channel axis with emissive probes. The influence of the heating current on the measured profiles is shown. (The position X = 0 mm refers to the channel exit plane.)

Langmuir probes are also made by our team using the same alumina tubes as for the emissive probes. The collecting surface consists of a 1 mm long and 0.2 mm diameter tungsten wire. The voltage sweep and current acquisition are done with an ALP Impedans control system. To extend the ±150 V sweep range of the ALP system, an additional DC power supply can be added in series between the probe and the acquisition system. This power supply is isolated via transformer and allows us to add up to 150 V of offset to the prob tip. Plasma potential was calculated from the current voltage (I-V) curve by finding the maximum of its first derivative. Light smoothing was done on this first derivative to isolate the maximum more precisely.

Both probe being of similar size, they have been mounted on the same fast translation stage.[28] This piezoelectric stage has a maximum acceleration of 2000 m/s$^2$ and a maximum speed of 350 mm/s over a 90 mm course. As seen on Fig. 3, it was used to move the probes in and out of the channel along the main axis of the thruster. All the data presented on this paper have been acquired along the center of the channel. While this system is not as fast as the ones used by Haas[29] (up to 2 m/s) or Staack[19] (1.5 m/s), its acceleration capabilities compared to most commercial systems can significantly reduce probe heating and pulverization. As a result, an increase in probe lifetime was observed.

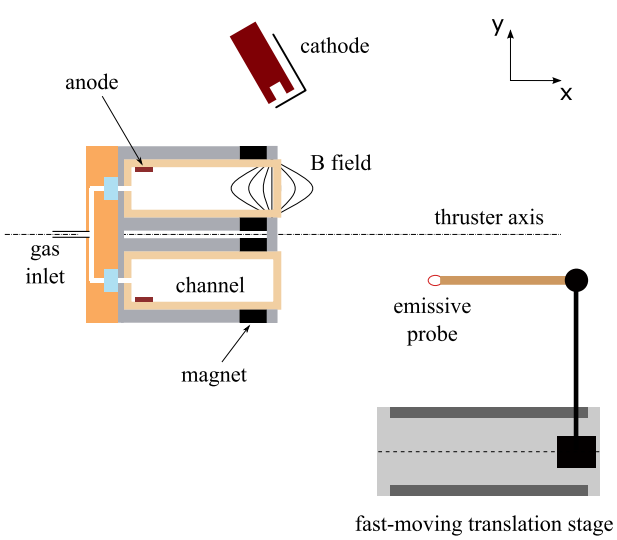


FIG. 3. Representation of the Hall thruster and probe translation stage installation. The probes travel along the thruster axis in the center of the discharge channel.

### C. LIF spectroscopy

Laser induced fluorescence is a complex technique that has already been extensively described in the literature, see Ref. 22 for a detailed description of the LIF technique applied to HT diagnostic. Only a brief overview is presented here.

A 834.72 nm laser beam is used to excite metastable $Xe^+$ ions. The ions which interact with the laser then fluoresce at 542 nm. When they are not at rest, the ions experience a Doppler shift that shifts the frequency of optical transition. By slightly changing the laser wavelength, specific ion velocity group can be made to fluoresce. By measuring the intensity of the fluorescence signal for each wavelength, the relative ion population of each velocity group can be determined. In our case, the axial velocity is probed by firing the laser at the center of the discharge channel. If simultaneous probe measurements are performed, the laser axis is positioned 3 mm away from probe axis, parallel to it, further along the circle defining the center of the discharge channel.

The IVDF is used to compute the electric field by calculating the potential drop ($\Delta V$) corresponding to the energy of the ions traveling at the most probable velocity measured ($v_{mpp}$),[30]

$$\Delta V = \frac{m_{ion} \cdot v_{mpp}^2}{2e}. \quad (1)$$

The electric field itself is computed by taking the derivative of the potential drop relative to the position (with a centered difference scheme).

This non-intrusive diagnostic does not disturb the discharge in any appreciable way as the power density injected in the measured volume is rather low (~1 mW/mm$^2$) compared to the discharge (in the order of 100 mW/mm$^2$).

## III. POTENTIAL DISTRIBUTION MEASUREMENT

### A. PPI - Low-power discharge

Measurements of the plasma potential with the three types of diagnostics have been performed on the PPI. Results with alumina and BN-$SiO_2$ walls are presented in Figures 4 and 5. No consistent measurement bias between optical and probe techniques is observed. Amplitude-wise the maximum of the electric field measured by LIF is either in the middle or below the probe results. Comparison between the position of the maximum is complicated since the LIF results in the $Al_2O_3$ case are very different from the ones given by the probe. This could be an indication of a change of the discharge mode. However both LIF and probes detect the "double peak" structure seen in this case. This double peak structure has already been observed by Vaudolon[31] and is currently unexplained.

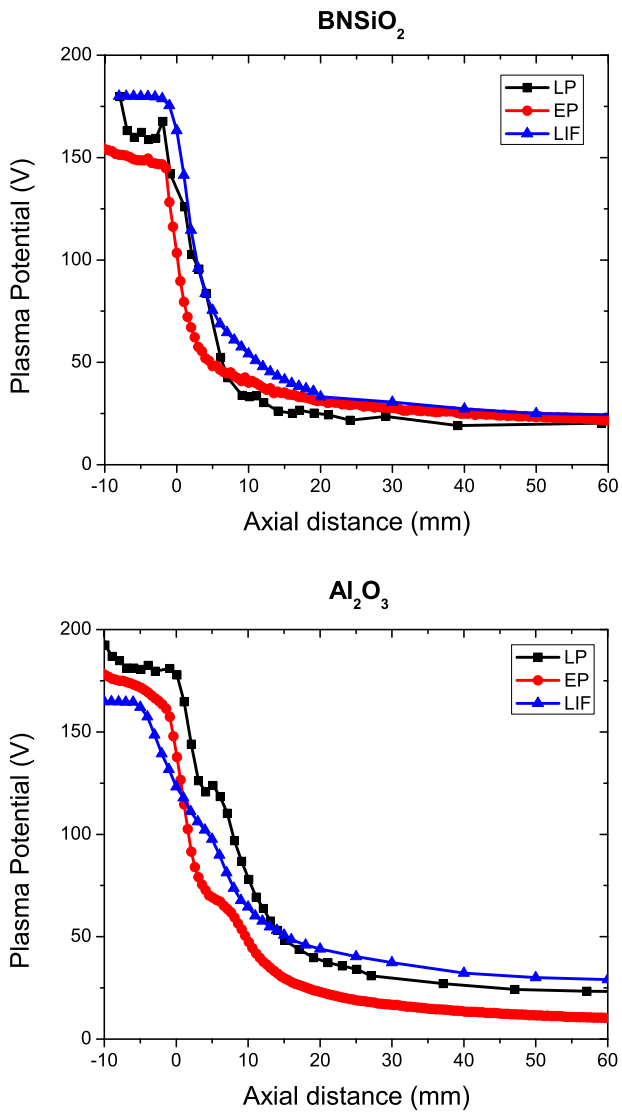


FIG. 4. Plasma potential along the channel axis of the PPI as measured by Langmuir probe (LP), emissive probe (EP), and LIF spectroscopy. The discharge was set at 200 V for 1 mg/s of xenon.

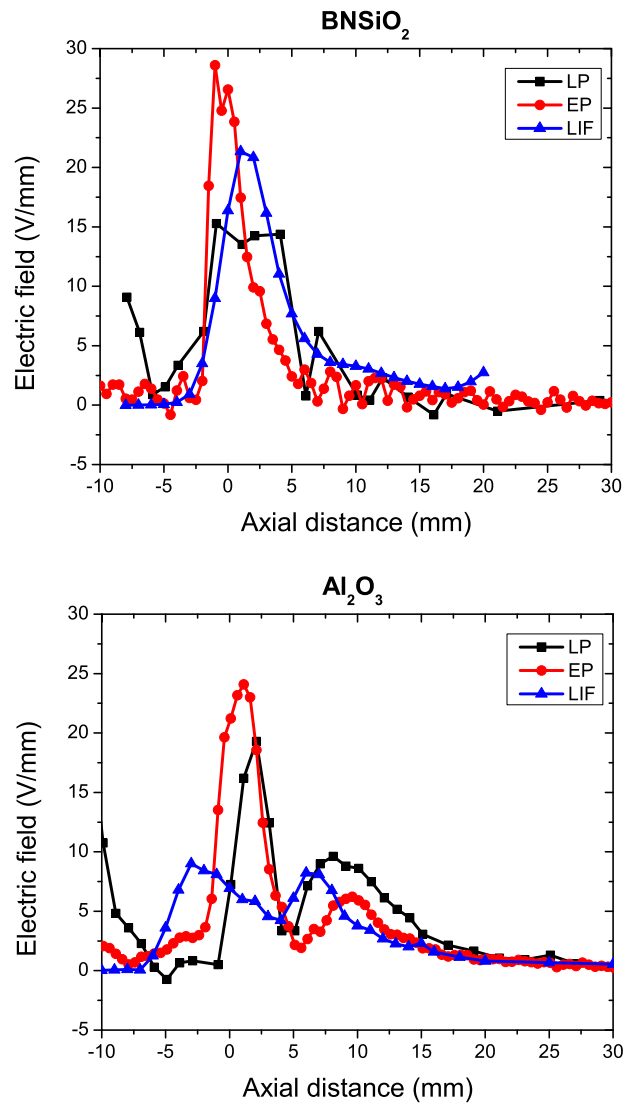


FIG. 5. Electric field along the channel axis in the PPI as measured by Langmuir probe (LP), emissive probe (EP), and LIF spectroscopy. The discharge was set at 200 V for 1 mg/s of xenon.

Looking only at the probe results, we see in both cases that the emissive probes measure a higher maximum for the electric field that is located further upstream. The difference is mostly seen inside the channel. The shift in position for the electric field is explained by the shift in position of the plasma potential measured by the emissive probe. A proposed explanation is that the emissive probe underestimates the plasma potential due to the fact that the emitted electron are colder than the plasma electron. The plasma potential being directly proportional to the electron temperature, a systematic error is expected inside the channel, where the electron temperature is high. The probe is also subjected to plasma heating that will increase the filament electron emissivity, effectively increasing the measured floating potential as if the heating current was increased.

Additionally the shear size of the tungsten loop makes measurement in the high potential gradient region imprecise. The design of the electrical circuit should provide us with the potential value of the middle of the loop. However inside the thruster, the plasma potential can change by as much as 100 V in less than 5 mm. Comparing this to the size of the probe (3 mm) explains the smoother curve obtained with the emissive probe. Moreover, as Haas[32] observed, the length of conducting tungsten placed in these low electron mobility regions appears to short-circuit the discharge.

The floating potential was also measured with both probes. Since in this case the emissive probe is left cold and effectively acts as Langmuir probes, both should give the same result. However the results in Figure 6 show completely different profiles once the probes are in the thruster. The main difference between the probes being the shape of the conducting tip, we assume that the discrepancy in the profiles is due to the length of the tungsten loop of the emissive probe (3 mm versus the 1 mm for the Langmuir probe). Moreover the alumina tube for the emissive probe has diameter of 4 mm (vs 2 mm for the Langmuir probe) which is significantly compared to the channel width of 10 mm of the PPI. Once again this highlights that the size issue emissive probes

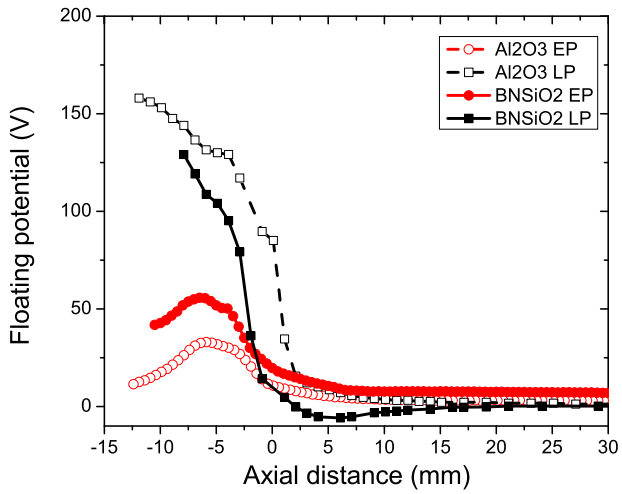


FIG. 6. Floating potential along the channel axis in the PPI as measured by Langmuir probe (LP) and cold emissive probe (EP). The discharge was set at 200 V for 1 mg/s of xenon.

have in high gradient environments such as the interior of a Hall thruster.

### B. SPT-100-ML - High-power discharge

Emissive probe and spectroscopy by LIF measurements in the channel of the SPT100-ML are shown in Figure 7. The electric field found with the probe is shifted roughly 5 mm upstream of the one found by LIF. This behavior has already been observed by Hargus.[11] A possible explanation raised to explain this results at the time was that the ion velocity was used in the LIF potential calculation. This choice gives less weight to the low velocity ion population and can thus be subject to errors in the ionization region. However our electric field, computed with the most probable ion velocity, shows a similar behavior. The choice of the most probable ion velocity is motivated by the results presented by Vaudolon[30] which point to this method giving the closest results to a true Boltzmann equation derivation.

This is further evidence that the difference between LIF and probe measurements are physical in nature, and not an artifact of the processing method.

## IV. PERTURBATIONS INDUCED BY THE PROBES

The results presented in III show that the probe measurement has an influence on the thruster electric field distribution. To further quantify the influence of emissive and Langmuir probes on the discharge characteristics, we have chosen to look at the local effect of the probe operation on the nearby ions velocity distribution. We also confirm through discharge current studies that the probes have a global effect on the discharge and that their perturbations are not confined to the electric field.

All the data presented in the following paragraphs have been collected on the PPI firing at a discharge voltage of 200 V and an anode mass flow rate of 1 mg/s.

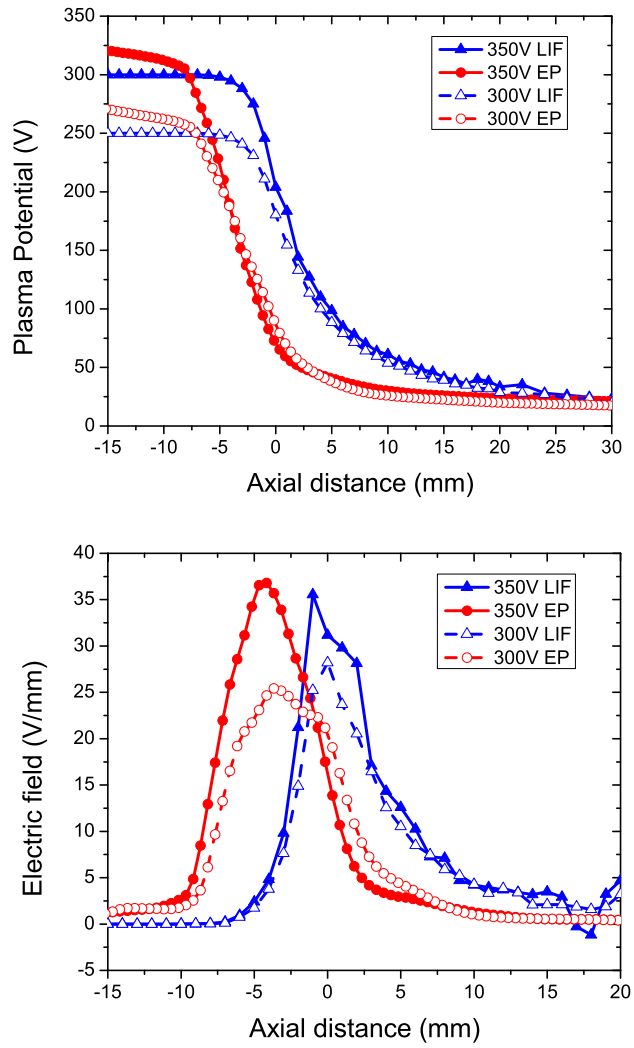


FIG. 7. Plasma potential and electric field along the channel axis in the SPT-100-ML as measured by Langmuir probe (LP), emissive probe (EP) and LIF spectroscopy. The discharge was set at 300 V for 3 mg/s of xenon.

### A. Emissive probes

Our emissive probe measurements with respect to the position along the channel axis are carried out during a back and forth "sweeping" motion of the translation stage. Figure 8 records the current during such a sweep. It is immediately apparent that the dynamics of the discharge current is very heavily influenced by the position of the probe. More precisely, the probe has no effect on the discharge while its tip is at more than 5 mm (half the channel width) from the exit plane of the thruster. Once it passes this threshold, the dynamics of the current are dramatically altered. While far from the thruster the current exhibits large asymmetric oscillations between +1.2 and −0.8 A of the mean value, the discharge suddenly changes to a more stable behavior with oscillations only 0.2 A in amplitude. This is also the position where the mean value of the current starts to increase. 5 mm upstream of the exit plane another more violent oscillating regime appears. These oscillations mean that value and amplitude are higher than in the undisturbed case. These transition regions appear about half a channel width upstream and downstream of the exit plane.

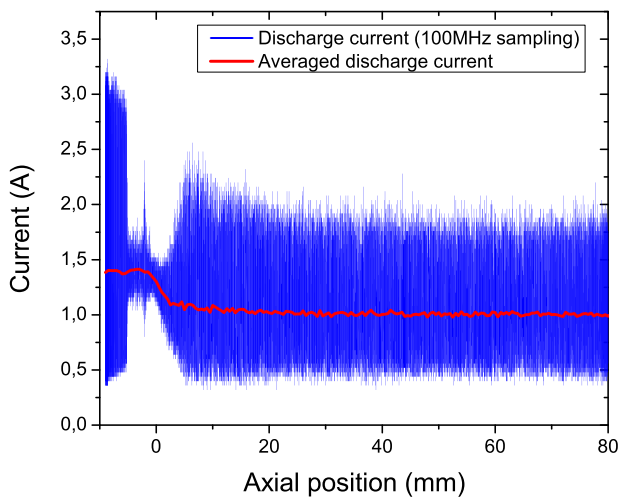


FIG. 8. Discharge current as a function of the emissive probe position in the PPI. The red line represents a moving average for readability. The current was acquired as the heated probe is translating at 250 mm/s toward the truster.

Figure 9 highlights the changes in discharge current dynamics as the probe is inserted. The figure is a spectrogram of the discharge current done by performing a fast Fourier transform over a short sliding window of sample points. Once again we find the same 3 discharge modes for $x > 5$ mm, 5 mm $> x > -5$ mm, and $x < -5$ mm. The principal mode of oscillations seen around 12 kHz in the undisturbed case completely disappears in the exit plane area before reappearing at a slightly lower frequency once the probe is inside the thruster. Note that the discharge current reacts very fast to the probe insertion. The probe goes through the "exit plane area" (5 mm to −5 mm) in only 50 ms but there is still a distinct discharge current behavior associated with this area.

This is slightly different from the behavior noticed with fast emissive probes by Staack[19] and Langmuir probes by Jorns.[33] In these studies, the perturbations only appeared once the probe was inside the thruster. Moreover, in Jorns' case, the average discharge current decreased as the probe was inserted. However the behavior change seen at −5 mm is around the same position (relative to the thruster channel size) as what Jorns observed. The difference in magnetic field topology (and thus electric field positioning) between the thrusters could explain the difference in behavior.

In order to see the local effect of the probe on the discharge, we have also measured the IVDFs by LIF at −5, 0 and 5 mm relative to the exit plane, with and without probes. Due to mechanical constraints, the LIF measurement point was positioned about 2 mm below and 1 mm upstream of the probe tip, but still at the center of the discharge channel. All the distances used in this experiment are relative to the probe tip (or where it would when be the probe was not used). Figure 10 presents the results we obtained. LIF acquisitions are relatively slow as the system needs a couple of minutes to cover the whole range of ion velocities. The longer residence time inside the thruster leads to heating of the alumina tube that can induce more side effects due to ablation of the tip of the probe as well as a change in the alumina dielectric properties. To account for this effects, acquisitions were also done with a non-heated intact emissive probe, a probe with a broken filament, as well as a simple alumina tube without one (Figs. 10 and 11). The probe with a broken filament was used to see if the residues left by a "burnt up" filament on the alumina tube had any effects.

The main perturbation effects are apparent when the probe is at the exit plane and is heated. The principal velocity group of ion is shifted to higher energy. Perturbations associated with the presence of a cold probe or a single alumina tube are also observed but are significantly weaker in comparison. The tungsten filament does not have an discernible effect by itself.

At 5 mm downstream of the exit plane, no significant perturbations are seen. This position correspond to where the transition on the current behavior happens in the PPI HT.

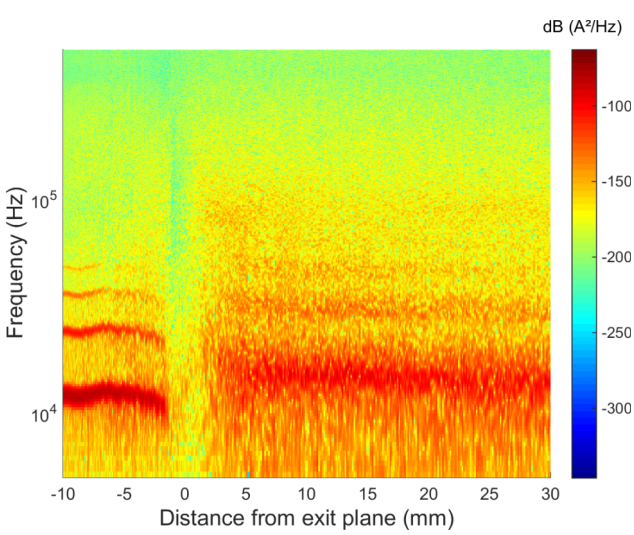


FIG. 9. Spectrogram of the discharge current as a function of the position of the probe in the PPI. The current was acquired as the heated emissive probe is translating at 250 mm/s toward the truster.

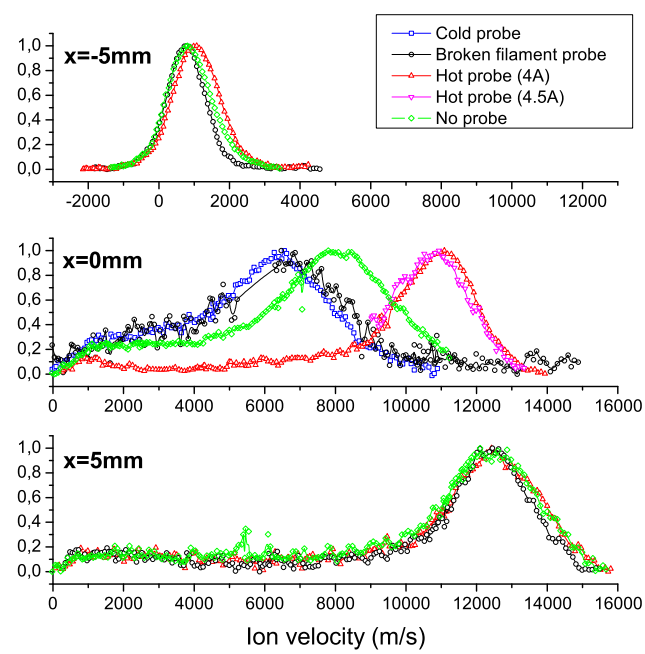


FIG. 10. IVDFs in the vicinity of the emissive probes inside (−5 mm), at the exit plane (0 mm), and outside (+5 mm) the PPI.

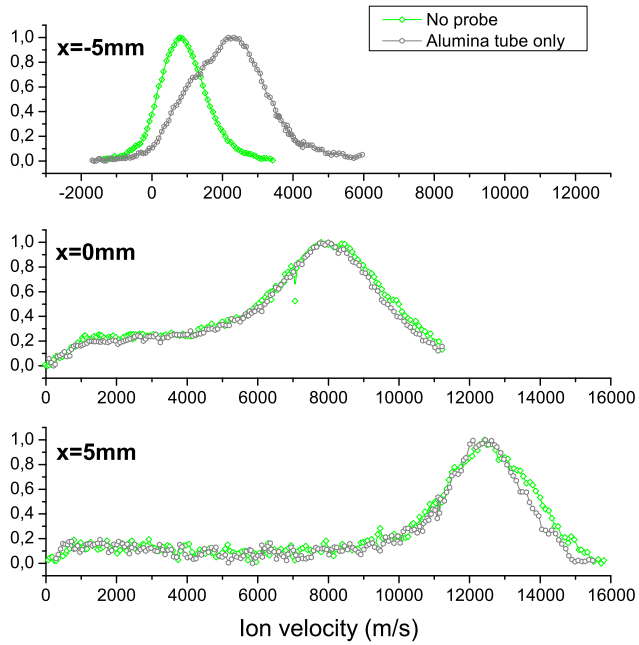


FIG. 11. IVDFs in the vicinity of the simple alumina tube inside (−5 mm), at the exit plane (0 mm), and outside (+5 mm) the PPI.

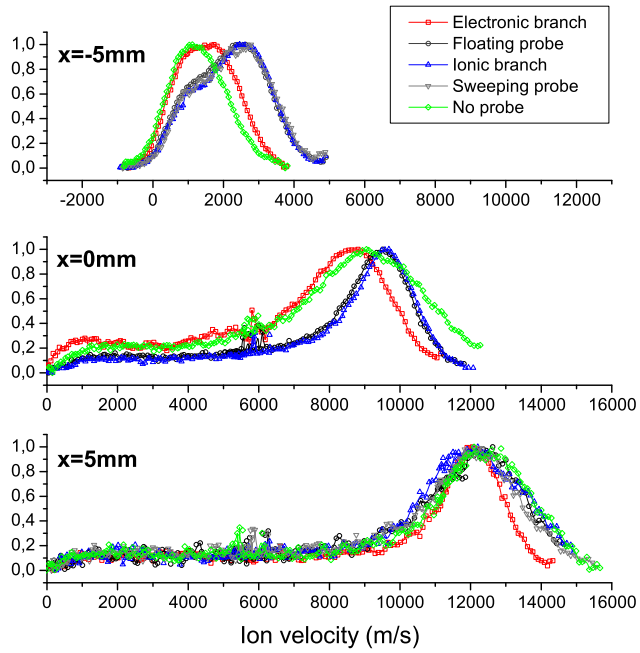


FIG. 12. IVDFs in the vicinity of the Langmuir probes inside (−5 mm), at the exit plane (0 mm), and outside (+5 mm) the PPI.

Furthermore the electric field at this point has already tapered off (see Fig. 5).

At −5 mm, the alumina tube gets "white hot" after about a minute inside the plasma. We also observe an increase of the discharge current as the probe gets hot. To preserve the thruster and the probe, LIF data acquisition was done during the transient regime. Due to this time sensitive effect, the replicability of the IVDF at this position was poor. However our data suggest that plasma heating of the alumina has a bigger effect than the probe heating. This is further supported in Section IV B when similar results are obtained using non-heated Langmuir probes.

The increase in both mean and most probable ion velocity is a good indication that the acceleration region and thus the electric field are displaced toward the anode by the probe.

### B. Langmuir probe

Similar LIF spectroscopy acquisitions have been performed with Langmuir probes. Since the main difference between them and emissive probes is the fact that they are polarized, we particularly looked at the influence of negative (ion collecting) and positive (electron collecting) polarizations relative to the plasma potential. We also did some sweeping probe measurements to simulate the situation when multiple I-V curves are recorded for averaging purposes.

As seen on Figure 12 at −5 mm relative to the exit plane the behavior is comparable to the one of the emissive probes. However when the probe tip is polarized positively, the most probable ion velocity is lower than in the other cases when the probe is present.

At the exit plane, we have a similar situation with three different type of IVDF. The one with a floating probe and a negatively polarized probe are once again shifted toward higher velocity compared to the undisturbed case. The positively polarized one has a most probable velocity close to the control case but the mean velocity is lower as there is less high energy ions.

At 5 mm downstream, the positively polarized probe shows a similar phenomenon while the floating and negatively polarized probes do not seem to induce any perturbations.

Probes with sweeping potential induce the same perturbations as negatively or floating probes for all positions.

## V. CONCLUSION

While inserting electrostatic probes in HT has be known to cause perturbations, we have presented here a direct comparison of the electric field measured with emissive probe, Langmuir probe, and non-intrusive LIF spectroscopy. A significant difference, mainly in position, is observed in both a small and medium sized HT.

By considering both discharge current and IVDF measurements at different probe position, we can identify 2 important factors in the perturbations. First the probes only start to have effect on the discharge when they get close to the exit plane of the thruster. This is seen both in the discharge current, with a threshold around 5 mm downstream of the exit plane, and in the IVDF where the probe effect starts to show up between 0 and +5 mm. This effect is present even when fast probing methods are used. The discharge reaction times seen in Section IV A shows that mechanical translation systems are unlikely to be ever fast enough to outrun these probe induced perturbations.

The second major factor seems to be the temperature of the alumina tube of the probe body. IVDFs of cold and hot probe tips show a distinct profile difference. Moreover this

could explain the position factor as probes gets hotter and hotter as they progress upstream.

This second phenomenon supports the concept of fast translating probe as a less invasive diagnostic method. A lower residence time inside the hot part of the discharge would not only preserve the lifespan of the probe tip but would also not let the alumina tube get hotter. Several properties such as conductivity[34] and secondary emissions are temperature dependent so the alumina at high temperature could be the source of the perturbations observed. Staack's[35] investigations show that these two properties have a major influence on the probe induced perturbations. He proposed and tested with good results several alternative materials (namely, segmented graphite and tungsten) for the probe body. Boron Nitride is also a good candidate as shown by Reid.[36]

In that respect, Langmuir probes should have less influence on the discharge as they are not heated. Their slightly longer measuring time compared to emissive probes (when a full voltage sweep is done) should be negligible as this electronic sweep can be made short enough (in the order of a millisecond) to fit within the minimum time it take to mechanically stop and start to retract the probe.

As a consequence, probe measurement inside and right of the exit plane of Hall thruster should be considered very carefully. On top of the already high errors on plasma properties associated with the important temperature gradient and strong magnetic field, the behavior of the discharge itself is significantly perturbed by the presence of the probes. Simulation validation and performance assessment should be done with data collected, thanks to non-intrusive methods such as LIF.

## ACKNOWLEDGMENTS

This work is part of the GIS PPE research program. It has been financially supported by the French space agency (CNES), the French Ministry of Science and the Région Centre.

[1]E. Ahedo, Plasma Phys. Controlled Fusion **53**, 124037 (2011).
[2]D. M. Goebel and I. Katz, *Fundamentals of Electric Propulsion: Ion and Hall Thrusters* (John Wiley & Sons, 2008), Vol. 1.
[3]V. V. Zhurin, H. R. Kaufman, and R. S. Robinson, Plasma Sources Sci. Technol. **8**, R1 (1999).
[4]I. D. Boyd, "Simulation of electric propulsion thrusters," Nato Report RTO-EN-AVT-194, paper 17 (University of Michigan, Ann Arbor, Michigan, USA, 2011).
[5]K. Dannenmayer, P. Kudrna, M. Tichý, and S. Mazouffre, Plasma Sources Sci. Technol. **20**, 065012 (2011).
[6]K. Dannenmayer and S. Mazouffre, Rev. Sci. Instrum. **83**, 123503 (2012).
[7]A. W. Smith and M. A. Cappelli, Phys. Plasmas **16**, 73504 (2009).
[8]L. Albarede, S. Mazouffre, A. Bouchoule, and M. Dudeck, Phys. Plasmas **13**, 63505 (2006).
[9]B. E. Beal, A. D. Gallimore, J. M. Haas, and W. A. Hargus, J. Propul. Power **20**, 985 (2004).
[10]B. E. Beal, A. D. Gallimore, and W. A. Hargus, Jr., Phys. Plasmas **12**, 123503 (2005).
[11]W. A. Hargus and M. A. Cappelli, J. Propul. Power **18**, 159 (2002).
[12]J. M. Haas and A. D. Gallimore, Phys. Plasmas **8**, 652 (2001).
[13]J. A. Linnell and A. D. Gallimore, Phys. Plasmas **13**, 93502 (2006).
[14]Y. Raitses, D. Staack, M. Keidar, and N. J. Fisch, Phys. Plasmas **12**, 057104 (2005).
[15]I. G. Brown, Phys. Fluids **14**, 1377 (1971).
[16]E. Passoth, P. Kudrna, C. Csambal, J. F. Behnke, M. Tichý, and V. Helbig, J. Phys. D: Appl. Phys. **30**, 1763 (1997).
[17]J. P. Sheehan, Y. Raitses, N. Hershkowitz, I. Kaganovich, and N. J. Fisch, Phys. Plasmas **18**, 073501 (2011).
[18]J. P. Sheehan, Y. Raitses, and N. Hershkowitz, in 33rd International Electric Propulsion Conference, Washington, DC, 2013.
[19]D. Staack, Y. Raitses, and N. Fisch, in *38th AIAA/ASME/SAE/ASEE Joint Propulsion Conference and Exhibit* (American Institute of Aeronautics and Astronautics, Reston, VA, 2002).
[20]F. F. Chen, J. D. Evans, and W. Zawalski, in *Plasma Diagnostic Techniques*, edited by R. H. Huddlestone and S. L. Leornard (Citeseer, 1965).
[21]I. Hutchinson, *Principles of Plasma Diagnostics* (Cambridge Univeristy Press, 2005).
[22]S. Mazouffre, Plasma Sources Sci. Technol. **22**, 13001 (2013).
[23]S. Mazouffre, G. Bourgeois, K. Dannenmayer, and A. Lejeune, J. Phys. D: Appl. Phys. **45**, 185203 (2012).
[24]A. Lejeune, K. Dannenmayer, G. Bourgeois, S. Mazouffre, M. Guyot, and S. Denise, in *Proceedings of the 32nd International Electric Propulsion Conference* (Wiesbaden, 2011), IEPC-2011-019.
[25]M. Touzeau, M. Prioul, S. Roche, N. Gascon, C. Pérot, F. Darnon, S. Béchu, C. Philippe-Kadlec, L. Magne, and P. Lasgorceix, Plasma Phys. Controlled Fusion **42**, B323 (2000).
[26]A. I. Morozov, in *23rd International Electric Propulsion Conference* (Electric Rocket Propulsion Society, 1993).
[27]S. Mazouffre, A. Petin, P. Kudrna, and M. Tichy, IEEE Trans. Plasma Sci. **43**, 29 (2015).
[28]A. Pétin, S. Mazouffre, K. Dannenmayer, P. Kudrna, and M. Tichỳ, in *Proceedings of the 33rd International Electric Propulsion Conference* (Electric Rocket Propulsion Society, 2013), pp. 1–14.
[29]J. M. Haas, R. R. Hofer, and A. D. Gallimore, in 35th AIAA/ASME/SAE/ASEE Joint Propulsion Conference, AIAA Paper No. 99-24, 1999.
[30]J. Vaudolon and S. Mazouffre, Phys. Plasmas **21**, 93505 (2014).
[31]J. Vaudolon, B. Khiar, and S. Mazouffre, Plasma Sources Sci. Technol. **23**, 022002 (2014).
[32]J. M. Haas, A. D. Gallimore, K. McFall, and G. Spanjers, Rev. Sci. Instrum. **71**, 4131 (2000).
[33]B. Jorns, D. M. Goebel, and R. R. Hofer, in *51st AIAA/SAE/ASEE Joint Propulsion Conference* (American Institute of Aeronautics and Astronautics, Reston, Virginia, 2015).
[34]M. Bauccio, *ASM Engineered Materials Reference Book* (CRC, 1994).
[35]D. Staack, Y. Raitses, and N. J. Fisch, Rev. Sci. Instrum. **75**, 393 (2004).
[36]B. Reid and A. Gallimore, in *44th AIAA/ASME/SAE/ASEE Joint Propulsion Conference and Exhibit* (American Institute of Aeronautics and Astronautics, Reston, VA, 2008).